Reversible coordination changes in crystalline silicates at high pressure and ambient temperature

G Serghiou†, R Boehler† and A Chopelas†‡

† Max-Planck Institute for Chemistry, Postfach 3060, Mainz 55020, Germany
‡ Department of Physics, University of Nevada, Box 454002, Las Vegas, NV 89154, USA

Abstract. In silicates, generally the less dense open structures of lower pressure polymorphs have four-coordinated silicon whereas the denser more close-packed structures have six-coordinated silicon. Transformation from the fourfold coordinated crystals to the denser sixfold coordinated structures upon compression usually requires an accompanying high temperature that is much greater than ambient. We report here a first-order, reversible SiO_4–SiO_6 coordination change in a crystalline silicate ($MgSiO_3$) orthoenstatite at ambient temperature and quasi-hydrostatic conditions using Raman spectroscopic measurements in a diamond cell to 70 GPa. Annealing experiments using a CO_2 laser, which controlled defect concentration, indicate that the four- to sixfold coordination change is facilitated by defects in the structure which may serve as nucleation sites for the formation of the octahedrally coordinated silicon phase.

1. Introduction

$MgSiO_3$ exists in a large variety of polymorphs which can be largely divided into two subclasses: (a) low-pressure modifications in which the Si is four-coordinated to oxygen and (b) high-pressure modifications in which the Si is six-coordinated. The low-pressure modifications contain SiO_4 tetrahedra and belong to the class of chain silicates (pyroxenes) which are also major components of the Earth's upper mantle [1]. The high-pressure modifications contain SiO_6 octahedra and have the ilmenite and the perovskite structures, the latter of which is considered the most abundant phase of the Earth [2, 3]. To date, transformations from tetrahedrally to octahedrally coordinated silicon phases of $MgSiO_3$ have only been observed after heating above about 1500 K at high pressure [4].

Previous ambient temperature four- to sixfold coordination changes of silicon upon compression have been observed in glasses (silica, sodium silicate and calcium aluminum silicate) using infrared and Raman spectroscopy [5, 6] and for silica using molecular dynamics simulations [7–9]. Transitions to crystalline silicate phases containing SiO_6 octahedra at ambient temperature and high pressure have only been reported for the quartz and cristobalite (a high-temperature polymorph of SiO_2) polymorphs of SiO_2 using x-ray diffraction and molecular dynamics simulations [10–12]. These observations are consistent with recent first principles energy calculations which generated a large number of octahedrally coordinated dense SiO_2 structures with similar enthalpies [13]. Quartz and cristobalite are fully polymerized in that the SiO_4 tetrahedra are all corner-linked to adjacent tetrahedra. While the SiO_2 system is an important prototype system for studying the crystal chemistry of silicates it does not contain some of the most important structural attributes characteristic of the majority of silicate structures, namely network modifier polyhedral units (MgO_x, CaO_x polyhedra).

Introducing network modifiers such as alkali or alkaline earth oxides into the structure breaks down the fully polymerized Si–O tetrahedral network because the oxygens are now shared with adjacent polyhedra containing network-modifying ions (countercations) which are typically octahedrally coordinated to oxygen. The bonding type also becomes more varied since the network modifier bonds to oxygen are less directional (more ionic) than the Si–O bonds within the tetrahedra [6].

We examine here whether coordination changes such as those seen for quartz and cristobalite are possible at ambient temperature when network modifying ions are present in the structure. Orthoenstatite ($MgSiO_3$) is orthorhombic with *Pbca* symmetry [14]. It consists of layers of edge sharing magnesium oxide octahedra which are separated from each other by chains of corner-linked (SiO_4) tetrahedra which are parallel to the crystallographic *c*-axis. The structural changes of $MgSiO_3$ upon compression at room temperature were monitored using Raman spectroscopy because this technique is a sensitive probe of four- to sixfold coordination changes [6]. Luminescence measurements were also performed to monitor possible changes in light emission due to the creation of defects near a coordination change. Separate CO_2 laser heating experiments were also performed to examine the effect of 'annealing' the structure (and thus minimize defect concentration) on its transition to a higher coordinated state.

2. Experimental techniques

Single crystals of orthoenstatite (Smithsonian No 137311) of end-member ($MgSiO_3$) composition were used for all experiments. Very weak red fluorescence emitted by the sample when excited with the argon-ion laser beam indicated the presence of trace amounts of Cr^{3+} ions occupying octahedral sites in the structure. The crystals of dimensions $10 \times 40 \times 40$ μm^3 were placed in the centre of 301 stainless steel gaskets in an argon medium. The sample chamber dimensions were between 130 and 150 μm in diameter and 60 μm in thickness. The Raman spectra were excited with the 457.9 nm line of an argon-ion laser with powers ranging from 5 to 30 mW. The Raman spectra were analysed with a Spex 1402 double monochromator with a LN-cooled CCD (charged coupled device detector). The luminescence spectra were excited using the 457.9 nm line of an argon-ion laser with 10 mW of power and measured in the wavelength regime of 470–770 nm using an HR320 single monochromator with a Photomultiplier tube. Heating of the samples was performed using the defocused beam of an 120 W continuous wave CO_2 laser [4]. Heating durations were about 20 min at temperatures of about 2000 K. Pressure was measured using micron sized ruby chips placed next to the sample.

3. Results

3.1. Raman measurements

The high-pressure Raman spectra of $MgSiO_3$ are shown in figures 1(a) (compression) and 1(b) (decompression). The ambient pressure spectrum of orthoenstatite spans the region from 200 to 1200 cm^{-1}. The vibrational modes can be classified into three regimes. The regime below 600 cm^{-1} consists of modes associated with countercation Mg–O stretches, internal O–Si–O bending, as well as longer wavelength lattice modes. The peaks in the mid-frequency region between 600 and 800 cm^{-1} are due to Si–O–Si inter-tetrahedral stretching and bridging modes, whereas the bands at higher wavenumbers are due to Si–O stretching modes of the non-bridging oxygens in the silicon tetrahedra [15].

We focus here on the compressional behaviour of the strong mid- and high-wavenumber modes, labelled with an 'o' in the ambient pressure spectrum in figure 1(a), because they are
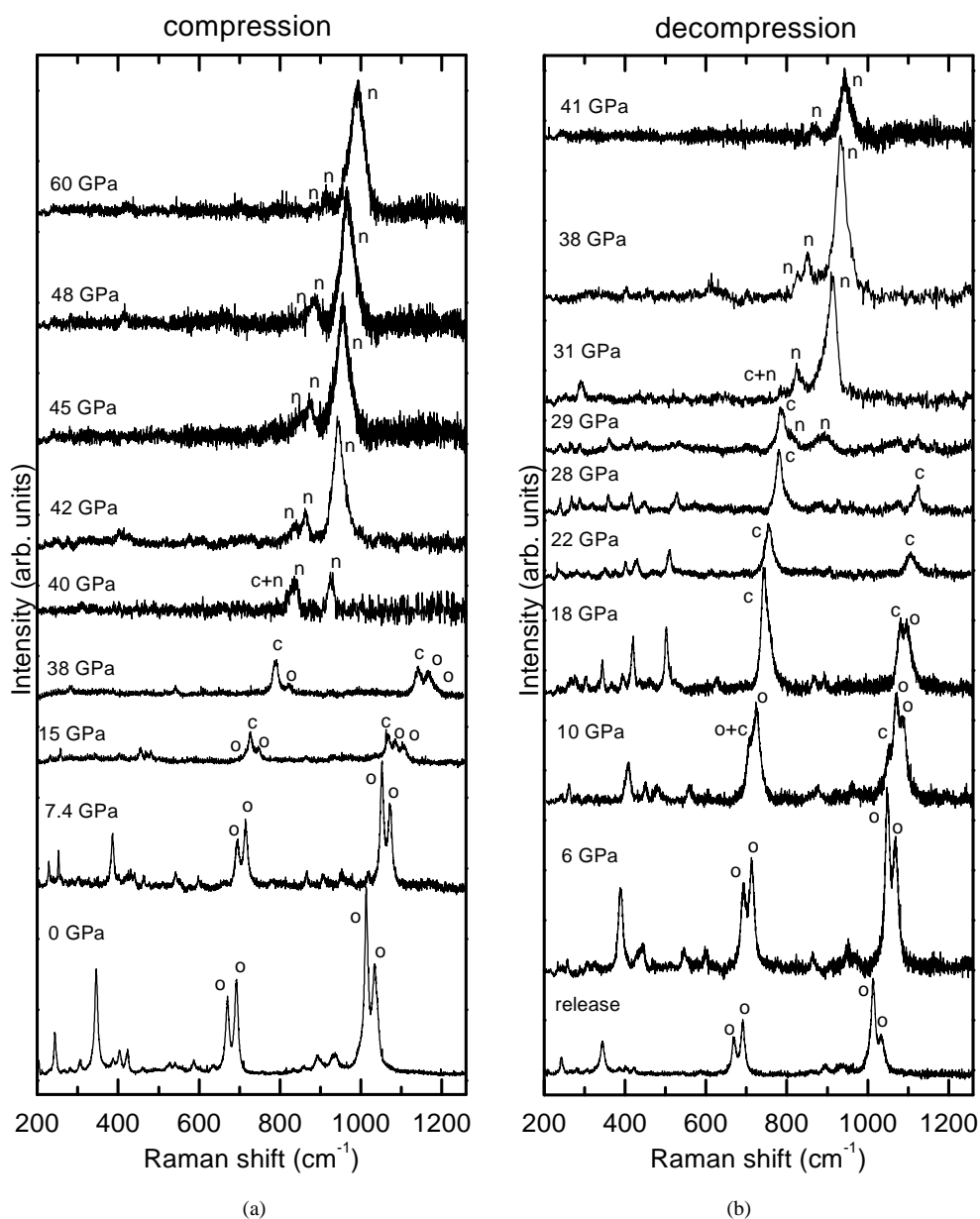
Figure 1. Effect of pressure on the Raman spectrum of orthoenstatite showing evidence for a reversible change of the coordination of silicon from four to six. The spectra in figure 1(a) are taken upon compression and the spectra shown in figure 1(b) are taken upon decompression. The peaks labelled with an 'o' represent orthoenstatite. The peaks labelled with a 'c' are from high-pressure clinoenstatite. The peaks labelled with 'n' are from the new six-coordinated high-pressure phase. We note that the feature (813 cm^{-1}) at 40 GPa can be traced to the residual lower pressure bridging mode in clinoenstatite, which undergoes a discontinuous jump in frequency at 40 GPa (figure 2(b)), becoming most likely a stretching vibration of silicon with a bridging oxygen in the SiO$_6$ unit in the new phase. The spectra shown are from several high-pressure runs on MgSiO$_3$.

most sensitive to coordination changes: two peaks are evident in both the central bridging mode region and the high-energy region because the orthopyroxene polymorph contains
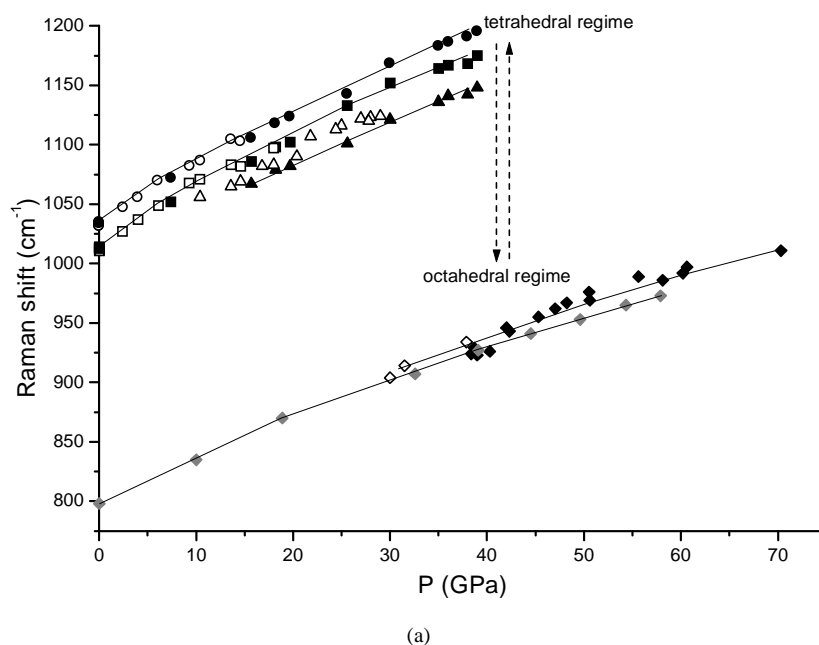
(a)

Figure 2. Frequency shifts of the most intense high-frequency (a) and mid-frequency (b) Raman bands during compression (filled symbols), and decompression (hollow symbols) through the transitions orthoenstatite–clinoenstatite–sixfold coordinated silicate structure. In figure 2(a) the squares and circles are from the strongest internal stretching modes of the tetrahedral units in orthoenstatite. The triangles are from the internal stretching vibration of the high-pressure clinoenstatite phase. The filled and hollow diamonds are from the strongest internal stretching vibration of the SiO_6 units in the octahedrally coordinated high-pressure structure. The grey diamonds are from the strongest internal stretching vibration of the SiO_6 units in ilmenite. In figure 2(b) the squares and circles are from the most intense Si–O–Si inter-tetrahedral bridging modes in orthoenstatite. The triangles up to 40 GPa are from the Si–O–Si inter-tetrahedral bridging mode of the high-pressure clinoenstatite phase and above 40 GPa from an internal stretching mode of silicon with a bridging oxygen within the SiO_6 units in the high-pressure octahedrally coordinated structure. The data shown are from several high-pressure runs on $MgSiO_3$. Data scatter is due to hysteresis and variation in the transition pressure on different runs (see text).

two crystallographically distinct chains. The observed pressure shift of Si–O–Si bridging modes to higher frequencies is associated with a closure of the inter-tetrahedral angle between corner-linked tetrahedra [16–18]. A closure of this angle together with distortions of the tetrahedral units are the principal mechanisms by which α-quartz as well as silica respond to increasing pressure [19], and is the structural pathway proposed for Si–O tetrahedral to octahedral coordination changes in silicate glasses [20, 21]. The two Si–O–Si vibrational modes associated with the two distinct chains in orthoenstatite shift by 26 cm^{-1} to 7 GPa (figure 2(a)). High-pressure single crystal x-ray diffraction measurements of orthoenstatite showed that the Si–O–Si inter-tetrahedral angles between the corner-linked tetrahedra decrease by (2.9°) and (2.1°), respectively, between 0 and 7 GPa [14]. Above this pressure, a mixed phase regime appears in accordance with previous single crystal Raman measurements [15], where the low-pressure orthoenstatite phase (*Pbca* space group) coexists with a high-pressure clinoenstatite phase (*C2/c* space group) as seen by the appearance of a Si–O–Si bending mode at 726 cm^{-1} and a Si–O stretching mode at 1067 cm^{-1} at 15 GPa, as shown in figure 1(a) (new peaks labelled with a 'c'). The lone Si–O–Si bridging and Si–O stretching modes
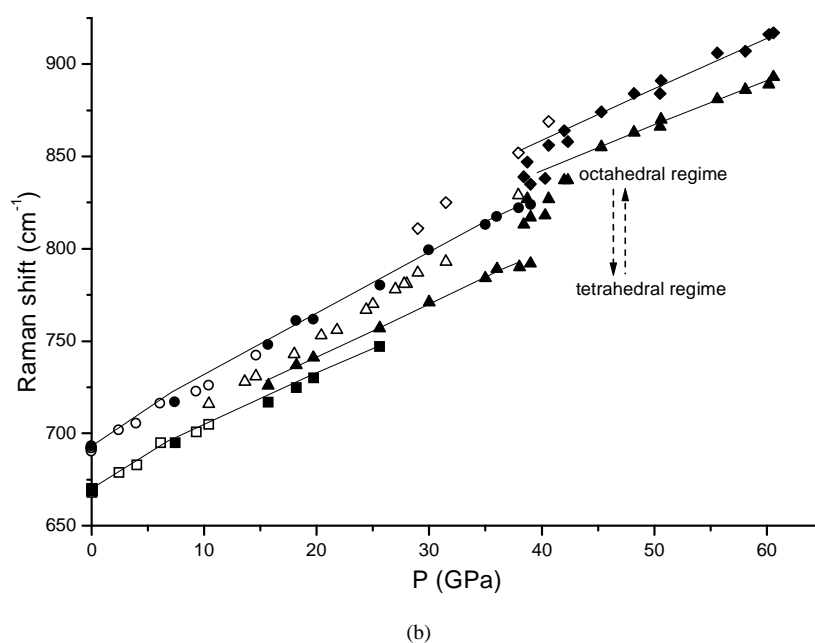
(b)

Figure 2. (Continued)

are representative of the one crystallographically distinct silicate chain in the high-pressure clinoenstatite in contrast to orthoenstatite which has two distinct chains [1, 22] and hence multiplet stretching (Si–O) and bridging (Si–O–Si) modes. The inter-tetrahedral Si–O–Si angle in high-pressure clinoenstatite is 121.6° at 8 GPa [1]. Geisinger *et al* [23] have shown that Si–O–Si tilting angles lower than 120° induce a sharp increase in strain energy of the Si–O–Si bond, making this structural configuration unfavourable. The Si–O–Si angle in clinoenstatite most likely becomes smaller than 120° at higher pressures. This assumption is based on the following consideration: the position of the Si–O–Si bridging mode of the clinoenstatite phase blue shifts by 65 cm^{-1} between 15 and 38 GPa (figure 2(a)). Both bond shortening and a decrease in the bending angle contribute to this blue shift. We note though that since a blue shift of 26 cm^{-1} between ambient pressure and 7 GPa of the Si–O–Si peaks in orthoenstatite corresponds to a closure of more than 2° of its inter-tetrahedral Si–O–Si angle, a blue shift of 65 cm^{-1} in the Si–O–Si peak of structurally similar clinoenstatite arguably reflects a closure of its Si–O–Si inter-tetrahedral angle by at least that much. This would result in an Si–O–Si angle in clinoenstatite of less than 120° at 38 GPa. An angle of 120° at 40 GPa is entirely consistent with recent *ab initio* molecular dynamics simulations of clinoenstatite, which find that at 30 GPa its Si–O–Si angle is 120.8° [24]. Extrapolation of the pressure dependence of this angle to 40 GPa yields 120°.

Between 39 and 40 GPa the frequency bands of the tetrahedrally (SiO$_4$) coordinated structure vanish and vibrational bands belonging to an octahedrally (SiO$_6$) coordinated phase appear (the peaks labelled with an 'n' are from the new phase) (figure 1(a)). The new Raman lines are broader than those of the lower pressure phases, which points to a significant degree of structural disorder in the new phase. We attribute the intense, highest wavenumber mode of the new phase to a stretching vibration of SiO$_6$ octahedral units, because its position and pressure dependency is very similar to that of the intense Si–O stretching vibration of SiO$_6$ units in MgSiO$_3$ ilmenite (figure 2(a)) [25]. In addition, octahedral stretching vibrations (SiO$_6$) in the
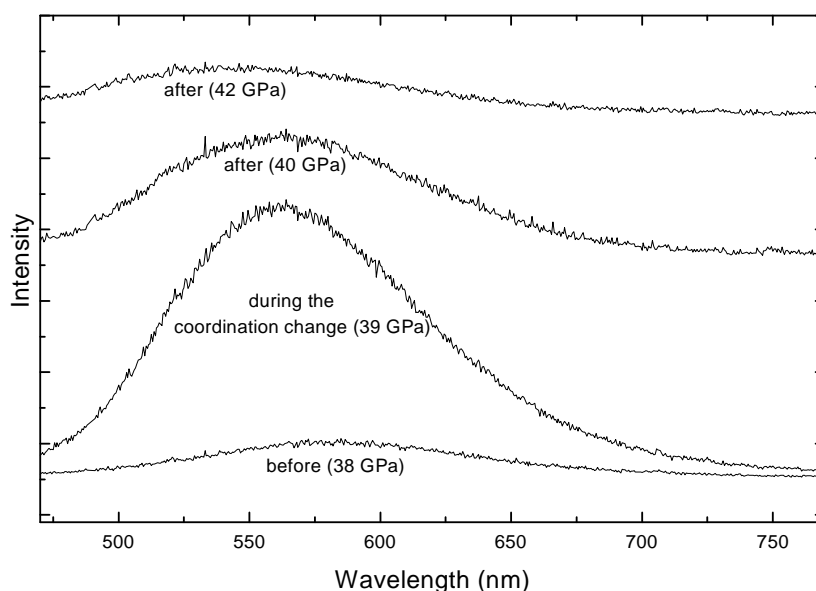
Figure 3. Luminescence spectra before (38 GPa), during (39 GPa) and after (40, 42 GPa) the transition to the high-pressure octahedrally coordinated structure. The luminescence spectra were measured using a Photomultiplier tube and were excited using the 457.9 nm line of an argon-ion laser with 10 mW of power.

same frequency regime have been observed in the infrared spectra of $MgSiO_3$ perovskite [26]. Based on the vibrational spectra of perovskite [26] and further studies on Raman vibrational mode assignments of ilmenite structures [27, 28], the bands at 813 and 840 cm^{-1} at 40 GPa are also attributed to stretching vibrations within the SiO_6 units (figure 1(a)). Mg–Si ilmenite and our new structure are similar in that they both contain SiO_6 units but they are not identical because the modes at 813 and 840 cm^{-1} do not appear in the ilmenite Raman spectrum. Proposed differences in the structures of ilmenite and the new phase are described in section 4.

Our new octahedrally coordinated structure remains stable to 70 GPa, the highest pressures of this study. Upon decompression (figure 1(b)), the new phase transforms back to clinoenstatite with a hysteresis of 9 GPa. The mixed ortho/clinoenstatite regime reappears at 18 GPa and the structure finally reverts back to the pure orthoenstatite phase below 10 GPa.

3.2. Luminescence measurements, laser heating and the role of defects

During the transition from the tetrahedrally to the octahedrally coordinated structure we observed a large increase in the luminescence intensity of the sample excited by the argon-ion laser beam between 470 and 770 nm (figure 3). As seen in figure 3, the luminescence intensity increases by about an order of magnitude at the transition pressure and decreases again after the transition to the pre-transition levels. We suggest that the luminescence stems from defect sites associated with broken bonds created during the coordination change, as well as electronic and structural changes at the impurity sites (such as chromium). Defect-induced luminescence bands have also been observed in fused silica at 477 and 669 nm [29], as well as upon compression of quartz at about 25 GPa—the pressure regime where it transforms to the higher coordinated quartz II structure which subsequently becomes amorphous [30, 31].
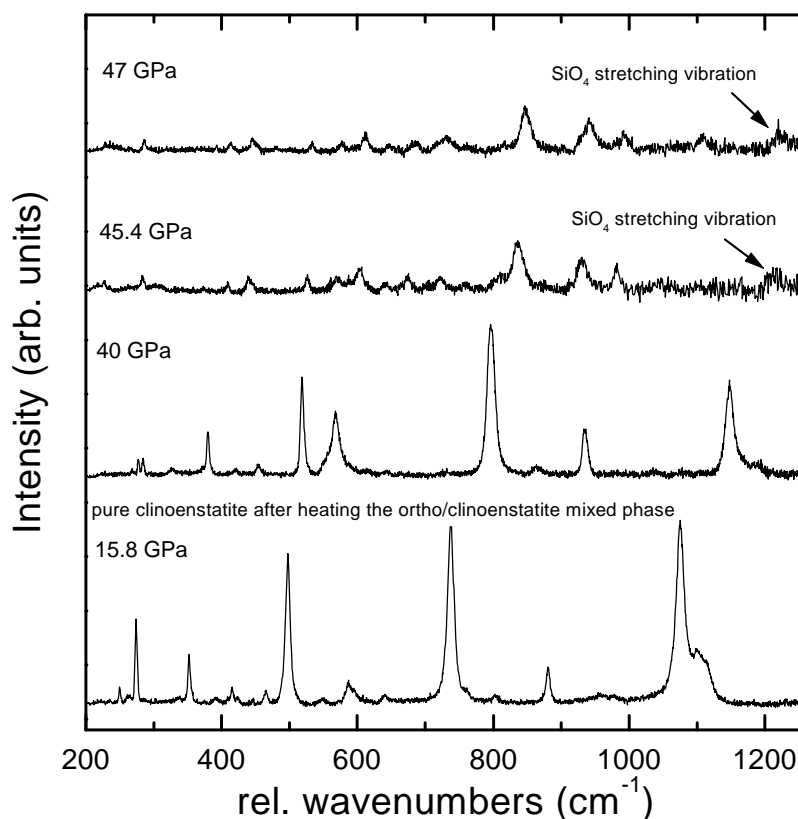
Figure 4. Effect of pressure on the Raman spectrum of clinoenstatite synthesized from the mixed ortho/clinoenstatite phase at 16 GPa, showing evidence for a phase transition above 40 GPa. Noteworthy is that the new phase exhibits a weak but clearly observable band which belongs to an Si–O tetrahedral stretching vibration (depicted by the arrow).

The creation of defects as well as the observed 9 GPa hysteresis indicates that the transition is first order. We found in further experiments that the four- to sixfold coordination change is time-dependent (examined 24 h later) and the transition pressure varies from 38 to 47 GPa. Time dependence as well as variation in transition pressure were also observed in previous high-pressure single crystal x-ray diffraction measurements of the first-order transition in another chain silicate ($FeSiO_3$), between the ortho and clinoferrosilite phases [32].

To examine whether defects promote the four- to sixfold coordination changes we synthesized pure clinoenstatite by heating the mixed ortho/clinoenstatite phase to 2000 K using a CO_2 laser at 16 GPa and measured the Raman spectra of the resulting pure clinoenstatite phase to 47 GPa. While a new phase appears above 40 GPa (figure 4), a weak vibrational mode above 1200 cm^{-1} is also present which is attributed to a Si–O tetrahedral stretching vibration. This is in contrast to the unheated $MgSiO_3$ experiments where the tetrahedral stretching modes vanished between 38 and 47 GPa. This observation indicates that defects present in the unheated $MgSiO_3$ structure provide nucleation centres that make the tetrahedral to octahedral transition more accessible. 'Annealing' the structure to the pure clinoenstatite phase minimizes or eliminates defects in the structure which arguably explains the persistence of tetrahedrally coordinated Si–O units in the new phase above 40 GPa. These defects or

nucleation centres then, make the four- to sixfold coordination change more facile. These defects likely appear in the form of grain boundaries at the interface between the ortho and clinoenstatite structures. They may also occur as local non-stoichiometries near the trivalent chromium sites. Local non-stoichiometries are required to preserve charge neutrality since the trace amounts of trivalent chromium substitute for Mg^{2+} ions in the structure.

4. Discussion

Linear extrapolation of the high-temperature phase boundary between ilmenite and perovskite (slope of $-0.0046\,GPa\,K^{-1}$) to 298 K [33] indicates that Mg–Si perovskite is the stable phase above 30 GPa at room temperature. Transition to perovskite though is kinetically impeded at the ambient temperature of our high-pressure experiments. In the absence of single crystal x-ray diffraction measurements, we cannot give a detailed description of the atomic rearrangements resulting in the high-pressure octahedrally coordinated phase we observe. Nevertheless, based on our Raman data, the mechanism of this first-order transition likely involves a tilting of the tetrahedral units towards each other within the chains, in accordance with the polyhedral tilt model developed to explain four- to six-coordination changes in silicate glasses [20]. This mechanism has also been reported to occur in the first-order phase transition of α-quartz to a higher coordinated crystalline phase under hydrostatic compression at 21 GPa [12]. Based on this polyhedral tilt model, the new high-pressure phase synthesized here consists of chains of edge sharing SiO_6 octahedra which differs both from (a) ilmenite which contains layers of edge connected Si–O octahedra and (b) perovskite which contains a three-dimensional network of corner connected Si–O octahedra. We note that layers of SiO_6 octahedral units can be formed by displacing the SiO_6 chains towards each other, perpendicular to their axis. This indicates that the layered ilmenite-type structure may be formed at high pressure from the octahedrally coordinated chain structure if the activation barrier for displacement of the chains towards each other is overcome at higher temperatures. This mechanism for formation of layers of SiO_6 units from chains is similar to that proposed for the high-pressure and temperature transition of clinopyroxene (chain structure) to ilmenite (layered structure) after shock impact [34].

Our study is important for modelling how low-density silicate crystals transform to their high-pressure octahedrally coordinated polymorphs because the transformations reported here occur at room temperature, are reversible and first order. Therefore the transformation mechanism can be narrowed down to models that do not involve large reconstructive changes. Furthermore, our results indicate that the presence of defects promotes the coordination changes upon compression and need to be considered in modelling these transitions.

References

[1] Angel R J, Chopelas A and Ross N L 1992 *Nature* **358** 322–4
[2] Finger L W and Hazen R M 1991 *Acta Crystallogr.* B **47** 561–80
[3] Knittle E and Jeanloz R 1987 *Science* **257** 668–70
[4] Boehler R and Chopelas A 1992 *High-Pressure Research: Application to Earth and Planetary Sciences* ed Y Syono and M H Manghnani (Tokyo: Terra Scientific Publishing Company) pp 55–60
[5] Williams Q and Jeanloz R 1988 *Science* **239** 902–5
[6] Wolf G H, Durben D J and McMillan P F 1990 *J. Chem. Phys.* **93** 2280–8
[7] Lacks D J 1998 *Phys. Rev. Lett.* **80** 5385–8
[8] Tse J S, Klug D D and Le Page Y 1992 *Phys. Rev.* B **46** 5933–8
[9] Jin W, Kalia R K, Vashista P and Rino J P 1994 *Phys. Rev.* B **50** 118–31
[10] Yamakata M and Yagi T 1997 *Proc. Japan. Acad.* B **73** 85–8
[11] Kingma K J, Mao H-K and Hemley R J 1996 *High Press. Res.* **14** 363–74
[12] Wentzcovitch R M, da Silva C, Chelikowsky J R and Bingelli N 1998 *Phys. Rev. Lett.* **80** 2149–52

[13] Teter D M and Hemley R J 1998 *Phys. Rev. Lett.* **80** 2145–8
[14] Hugh-Jones D A and Angel R 1994 *Am. Mineral.* **79** 405–10
[15] Hugh-Jones D, Chopelas A and Angel R 1997 *Phys. Chem. Min.* **24** 301–10
[16] Furukawa T, Fox K E and White W B 1981 *J. Chem. Phys.* **75** 3226–37
[17] Fleet M E and Henderson G S 1995 *J. Solid State Chem.* **119** 400–4
[18] Matson D W, Sharma S K and Philpotts J A 1983 *J. Non-Crystalline Solids* **58** 323–52
[19] Hazen R M, Finger L W, Hemley R J and Mao H K 1989 *Solid State Commun.* **72** 507–11
[20] Stolper E W and Ahrens T J 1987 *Geophys. Res. Lett.* **14** 1231–3
[21] Jeanloz R 1988 *Nature* **332** 207
[22] Sueno S and Prewitt C T 1983 *Fortschr. Min.* **61** 223–41
[23] Geisinger K L, Gibbs G V and Navrotsky A 1985 *Phys. Chem. Min.* **11** 266–83
[24] Wentzcovitch R M, Hugh-Jones D A, Angel R J and Price G D 1995 *Phys. Chem. Min.* **22** 453–60
[25] Reynard B and Rubie D C 1996 *Am. Mineral.* **81** 1092–6
[26] Lu R, Hofmeister A M and Wang Y 1994 *J. Geophys. Res.* **99** 11 795–804
[27] Baraton M I, Busca G, Prieto M C, Richiardi G and Sanchez Escribano V 1994 *J. Solid State Chem.* **112** 9–14
[28] Busca G, Ramis G, Gallargo Amores J M and Sanchez Escribano V 1994 *J. Chem. Soc. Faraday Trans.* **90** 3181–90
[29] Silin A R, Skuja L N and Trukhin A N 1980 *J. Non-Crystalline Solids* **8** 195–200
[30] Kingma K J, Meade C, Hemley R J, Mao H-K and Veblen D R 1993 *Science* **259** 666–9
[31] Hemley R J 1998 *Ultrahigh-Pressure Mineralogy* vol 37 (Washington, DC: Mineralogical Society of America)
[32] Hugh-Jones D, Sharp T, Angel R and Woodland A 1996 *Eur. J. Min.* **8** 1337–45
[33] Chopelas A 1999 *Am. Mineral.* **84** 233–44
[34] Tomioka N and Fujino K 1997 *Science* **277** 1084–6